

Electronic excitations in SnS_2 : An electron-energy-loss-spectroscopy study

H. Cohen

*Solid State Institute, Technion-Israel Institute of Technology, Haifa 32000, Israel
and Physics Department, Technion-Israel Institute of Technology, Haifa 32000, Israel*

M. Folman and T. Maniv

*Solid State Institute, Technion-Israel Institute of Technology, Haifa 32000, Israel
and Chemistry Department, Technion-Israel Institute of Technology, Haifa 32000, Israel*

R. Brener

Solid State Institute, Technion-Israel Institute of Technology, Haifa 32000, Israel

E. Lifshitz and Z. Esterlit

*Solid State Institute, Technion-Israel Institute of Technology, Haifa 32000, Israel
and Chemistry Department, Technion-Israel Institute of Technology, Haifa 32000, Israel*

(Received 27 November 1991)

A reflection-electron-energy-loss spectroscopy study of $2H\text{-SnS}_2$ single crystals is presented. Low-energy losses, traditionally attributed to single-electron transitions, are shown here to be of a collective character. Their interpretation as collective eigenmodes of a multiplasma electronic system is demonstrated with the aid of a simplified two-plasma model, which yields a remarkably good agreement with the experimental data. Within this framework, some of the distinct differences between the various modes are emphasized. Their hybrid (bulk and surface) behavior, as well as the physical origin of the shifts of electron losses, with respect to optically detected peaks, are coherently explained. A comparison with complementary SnS_2 studies is also used for the identification of single-electron transitions from core levels. The existence of a tightly bound exciton, localized on the Sn atoms, is confirmed. Its binding energy is determined here as 1.5 eV, a value extracted from comparing various techniques having different sensitivity to local effects.

I. INTRODUCTION

The dichalcogenides have been a subject of many studies during the last decades. Their quasi-two-dimensional structure, and the ability to control their optoelectronic properties by intercalation, have stimulated intensive basic as well as applicative research. Being very convenient for vacuum handling, a relatively large number of surface techniques has been applied to these materials, including electron-energy-loss spectroscopy (EELS), which has already been proven¹⁻⁴ to be a powerful technique for the study of electronic properties.

One of the widely studied dichalcogenides is SnS_2 , and its $2H$ polytype⁵ in particular. Its electronic structure was calculated,⁶⁻¹¹ and measured by optical absorption,¹² optical reflection,¹³⁻¹⁸ ultraviolet photoemission spectroscopy (UPS),¹⁹⁻²¹ constant-initial-state spectrum (CIS),²²⁻²³ x-ray photoemission spectroscopy (XPS),²⁴⁻²⁶ bremsstrahlung isochromat spectroscopy (BIS),²⁷ and transmission EELS (TEELS).²⁸ Very recently, reflection-EELS (REELS) studies of this compound have also been published.^{29,30} Yet there is no coherent understanding of this compound. Applying REELS to SnS_2 , and taking the advantage of that large amount of data, our purpose here is to gain a better understanding of the nature of loss

features, as well as the related electronic structure of SnS_2 .

EELS is best suited for collective electron excitation characterization. As the primary energy is varied through the sub-keV region, a clear distinction between bulk and surface plasmons is available. The bulk plasmons, having ideally a zero amplitude outside the material, can only be excited via the penetration of the probing electron beyond the surface, a stage which is highly dependent on the primary energy E_0 . Their intensity in the loss spectrum is, therefore, significantly increased with increasing E_0 . On the other hand, the surface plasmon amplitude exponentially decays into the vacuum, having, at long wavelengths, a long-range interaction with the external electron, and a weak E_0 dependence.

A loss peak, with an apparent bulk-plasmon character, which does not obey the expected E_0 dependence, has therefore drawn our attention, and is discussed in this paper in detail. The change in the effective-momentum transfer, involved in the primary energy variation, is also discussed and examined. A simple model, consisting of two independent plasmas, is used to describe the collective modes, yielding an excellent agreement with the dominant loss features,³⁰ and elucidating some unusual

surface properties.

Our REELS results are compared with the various works mentioned above, aiming at clarifying the discrepancies found between the results of different techniques, and demonstrating some advantages of EELS as a complementary tool. This also concerns the transitions from the $\text{Sn}(4d)$ core levels. The results verify the existence of very strong correlation effects, reflected in extremely large excitonic binding energies.

II. EXPERIMENT

SnS_2 samples were prepared by the chemical vapor transport technique, using iodine as a carrier, and elemental S and Sn powders (purity 99.999%). The above materials were put in an evacuated quartz ampule, and heated to 700°C in a two-zone furnace, maintaining a 50°C temperature gradient along the tube. The process was carried out for eight days, in order to minimize the creation of defects. The samples obtained were yellow-brown platelets of $50\text{--}100\text{-}\mu\text{m}$ thickness, and about $5\text{--}10\text{-mm}$ plane size.

An x-ray analysis gave a high-quality trigonal single-crystal picture, classified as $2H$, with primitive axes of $a=b=3.651\text{ \AA}$ and $c=5.90\text{ \AA}$. No evidence has been found for any mixing of other known polytypes of SnS_2 .⁵ It should be recalled that the $1T$ structure, with symmetry group $P\bar{3}m1$, has been mistakenly called $2H$, for the CdI_2 structure group of materials.³¹ We adopt this notation here, too.

Surface quality was determined by scanning electron microscopy (SEM), XPS, and Auger electron spectroscopy (AES). Using SEM we established the existence of

large, flat, homogeneous areas before and after cleavage. No traces of foreign surface contaminants (including iodine) were detected by XPS or AES except for a small amount of carbon. This could be avoided by cleaving the sample in atmosphere just before insertion into the vacuum chamber. In fact, the spectral features shown below were found to be insensitive to the carbon presence.

EELS measurements were performed at room temperature and a base pressure of 3×10^{-10} Torr, in a commercial Perkin Elmer PHI model 555 ESCA-Auger system, using beam energies in the range of $80\text{--}2000\text{ eV}$, and beam currents of $50\text{--}100\text{ nA}$. The incident beam was directed at an angle of 40° from the normal to the surface (the c axis). A double-pass cylindrical mirror analyzer (CMA) was used to analyze the electrons, scattered into a cone of 42.3° with respect to the primary beam.

Most of the measurements were taken in the retarding grid mode, yielding $N(E)/E$ spectra. Numeric differentiation was used for fine-structure treatments. The alternative first-derivative modulation mode (1 V peak to peak) gave the same results, usually with a lower resolution. In the $N(E)$ mode, using a low-pass energy of 15 eV , a 0.2-eV resolution was obtained at all primary energies, and even a value of 0.1 eV could be achieved under special conditions. This improved resolution makes the conventional system competitive with various techniques, including CIS and BIS.

III. RESULTS AND DISCUSSION

The EEL spectra of SnS_2 and their second derivatives, presented in Fig. 1, show several narrow lines up to the 9.0-eV loss, a couple of broad bands, finely structured

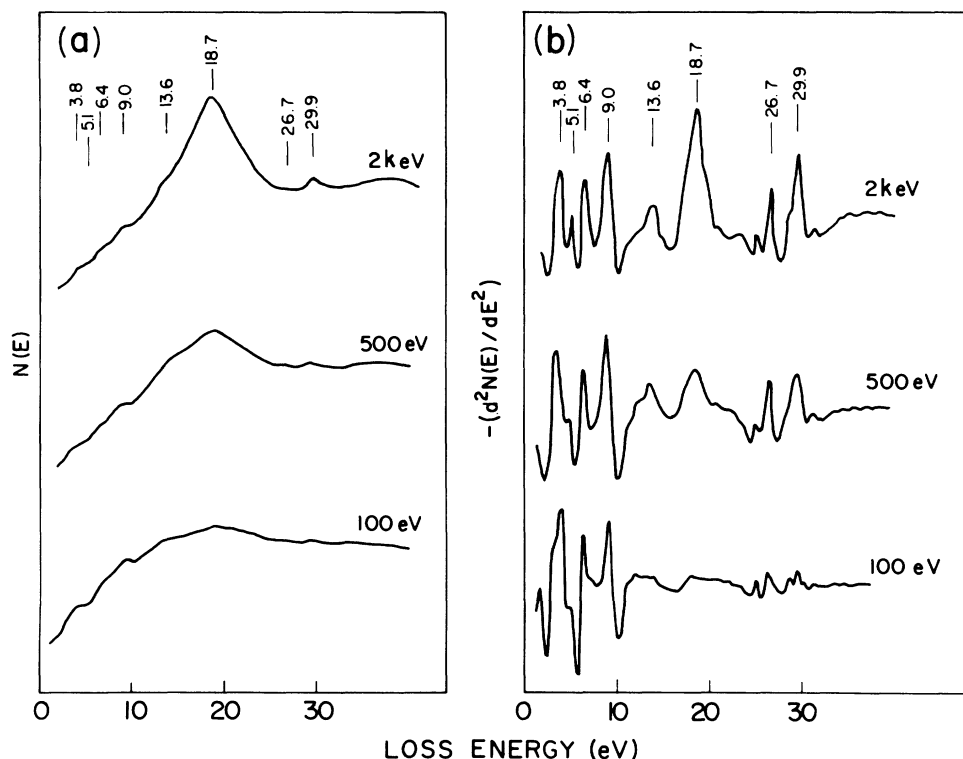


FIG. 1. Loss spectra at representative primary energies: (a) intensities; (b) second derivatives.

within the range of 10–25 eV, and an additional doublet of sharp lines at about 26.7 and 29.9 eV. As a whole, no additional peaks or energy shifts were observed by varying the beam energy through the entire E_0 range. The influence of E_0 was mainly expressed in changes of relative intensities within the central region.

These spectra agree fully with the data of Ohno,²⁹ and with the single REEL spectrum published by Ohuchi *et al.*,³² except for some additional fine details observed here due to better resolution. The assignment of the coupled broad bands to the bulk and surface plasmons of the valence electrons is widely accepted.^{28–30} The narrow low-energy lines have been previously attributed to single-electron interband transition,²⁹ as well as the lines just below 30 eV, which were proved^{17,18} to be related to transitions from the Sn(4*d*) levels. For part of these spectral features, an alternative interpretation is suggested here. In Secs. III A and III B, we discuss the nature of the features by (a) identifying the collective excitations and (b) using the single-electron transitions, originated in the Sn(4*d*) core level, to extract information about the unoccupied levels (the conduction bands).

A. Collective excitations

1. The dominant plasmon

The bulk plasmon of the total 16-valence electrons is easily identified as the broad line around 18.7 eV: This line, as well as its first harmonics, is dominant in the $N(E)$ representation, and shows a strong intensity dependence on the primary energy E_0 —a clear indication of a bulk collective excitation [see Fig. 1(a)].

The expected energy for this mode is somewhat lower. A value of 18.1 eV is obtained from the free-electron relation

$$\omega_{p_0}^2 = 4\pi n e^2 / m, \quad (1)$$

where n is the electron concentration and m and e are the free-electron mass and charge, respectively. For bound electrons, where the binding energy is of the order of the energy gap E_g , a small correction is expected,³³ resulting in $\hbar\omega_p \approx 18.25$ eV. This latter value agrees with TEELS measurements,²⁸ and is also obtained by the Kramers-Kronig analysis of optical-reflection measurements.^{14,18}

We think that the above difference between the measured values is significant—though small—and is caused by plasmon dispersion. Our experimental configuration reveals a weighted integration over a wide q range, due to the integration over wide angle. Following the analysis of Ohno,¹ dominant contributions should appear from the $q_m/3$ to $3q_m$ range, where q_m is the magnitude of the most probable transferred wave vector. For an isotropic sample, it is found that with $E_0 = 2$ keV, q_m is approximately 0.15 \AA^{-1} , while at $E_0 = 100$ eV, q_m is almost 0.8 \AA^{-1} . For the extreme anisotropic case, q_m can be changed by a factor of $\sqrt{2}$, leading, for example, to about 1 \AA^{-1} at $E_0 = 100$ eV.

The importance of nonzero q values in our measured plasmon band is proven by the comparison with the data

of Manzke, Fink, and Creselius,³⁴ who measured this dispersion by means of TEELS. The extrapolation of these results to $q = 0$ gives $\hbar\omega_p \approx 18.3$ eV, resembling the values mentioned above. One finds a close similarity between their higher- q spectra and our low- E_0 ones. We therefore believe that $q > 0$ plasmon excitations dominate the 19–24-eV-loss range, broadening asymmetrically the 18.7-eV peak toward its high-energy side. This last argument should be valid also for $E_0 = 2$ keV, and certainly for $E_0 = 100$ eV.

One should distinguish between two phenomena, which affect the plasmon band intensity, when the primary-beam energy is reduced: An increase of q_m and a decrease of the penetration depth. For increasing values of q , when q exceeds the critical value for Landau damping, the plasmon lifetime should be significantly reduced. The other effect is the excitation cross section, which is strongly dependent on the penetration of the external electron into the material. As can be verified by the comparison with the data of Manzke, Fink and Creselius, the latter effect is dominant in REELS, at least above $E_0 = 200$ eV.

An asymmetric broadening toward the low-energy side is expected when the dielectric function is anisotropic. In principle, when the wave vector coincides with the z axis, the corresponding plasmon frequency ω_z is usually smaller than the in-plane plasmon ω_{xy} , due to the lower effective mass within the plane of the layers. However, for an arbitrary direction (defined by its angle with the z axis, α), the relevant nonrelativistic mode is given by³⁵

$$\epsilon_{xy} \sin^2 \alpha + \epsilon_z \cos^2 \alpha = 0, \quad (2)$$

and the integration of the analyzer over the various directions, leads to a continuous crossover between ω_{xy} and ω_z . Recalling that the values mentioned above^{14,18,28} are all concerned with in-plane q vectors, one may estimate an upper limit of about 2 eV for the anisotropy of ω_p , while in graphite, ω_z is almost 7 eV lower than ω_{xy} . The question of anisotropy will be raised later again. At this stage we would like to draw attention to the similarity of the present case to other dichalcogenides, such as MoS₂, where the anisotropy of the plasmon energy is of about 0.5–1.0 eV.³⁶

2. Additional plasmons

We shall now focus on the 9.0-eV line, which has an overall appearance of an intensive interband transition; it is relatively narrow and, more importantly, it does not show any remarkable intensity dependence on the primary energy, including the 80-keV region measured by TEELS.²⁸ Yet, its nature should be discussed in view of the following facts.

(1) No justification of a specially intensive interband transition around 9.0 eV has been found in the various band calculations.^{6,9,10}

(2) Optical-reflectivity measurements^{13–15,18} also lack any observable peak at this energy and show, in fact, a strong dip at about 9.5 eV. This dip was attributed, by Raisin, Bertrand, and Robin,¹⁵ to the presence of a gap in

the optically allowed transitions. The minimum in the calculated, as well as the experimental, joint density of states (DOS) is, however, much less pronounced than the reflectivity dip. In our opinion, the above-mentioned structure around 9.0 eV is, simply, the typical appearance of a plasma edge in the optical reflectance, related to an additional bulk plasmon. Such an interpretation is also consistent with the $q=0$ dielectric function calculated from those measurements,^{14,18} where $\text{Re}(\epsilon)$ approaches zero at this energy.

(3) The existence of couples of valence-band bulk plasmons is well known in layered materials like graphite or transition-metal dichalcogenides (TX₂). Such a couple of modes is explained by the existence of two separated valence bands. The lower-energy mode is frequently attributed to the collective oscillation of electrons in the higher-valence band (the π electrons), while both valence bands are considered to create the higher-energy plasmon.²⁸

As suggested in Ref. 28, the participation of d electrons in the valence band of TX₂ can explain the observed couple of modes in TEELS measurements. Liang and Cundy²⁸ did not, however, apply this mechanism to SnS₂, having no evidence of a twofold valence-band structure. Later works, however, evidently showed, both theoretically³⁷ and experimentally,²⁴ the existence of two separated bands. In Fig. 2, the valence-band DOS function is presented in the manner of Simunek and Wiech,³⁷ being in overall agreement with the other works mentioned above. It consists of two bands, the first having four major maxima (1V–4V), and the second being dominated by a sharp peak and a broad shoulder (5V–6V). The dominant atomic-orbital character of these struc-

tures is indicated too. Similarly, the conduction-band DOS is illustrated in the manner of Bordas, Robertson, and Jakobsson,¹⁸ having, however, a poorer agreement in details with other calculations (see the discussion in Sec. III B).

The above facts clearly favor the collective-mode interpretation of the 9.0-eV loss over the single-electron excitation. Moreover, this interpretation can be quantified by using a simple model of two independent plasmas coupled through the common electric field.

In this framework the dielectric function is given by³³

$$\epsilon = 1 - \sum_j \omega_{pj}^2 / (\omega^2 - \omega_{nj}^2 + i\omega\delta_j), \quad (3)$$

where $\omega_{pj}^2 = 4\pi n_j e^2 / m_j^*$ with n_j and m_j^* being the j th plasma's electron concentration and effective mass, respectively; $\hbar\omega_{nj}$ is an effective binding energy of the j th oscillator and δ_j is its damping parameter.

Clearly, when only two plasmas are involved, two modes are created: A symmetric mode (ω_+), in which the two plasmas oscillate in phase, and an antisymmetric mode (ω_-) consisting of an antiphase oscillation.

In terms of this dielectric function, the loss intensity I is written here as a superposition of surface and bulk loss functions,

$$I \sim \text{Im} \left[-\frac{1}{(\epsilon+1)} \right] + D \text{Im} \left[-\frac{1}{\epsilon} \right], \quad (4)$$

with $D(E_0)$ as a phenomenological parameter. The values of the parameters used are given in Table I.

This set of parameters has been obtained by the following fit procedure. We first assumed δ_j to equal zero, and found analytically the four parameters ω_{pj} and ω_{nj} by inserting the experimental frequencies for the roots of the equation $\epsilon=0$. Since only three of the measured frequencies were easily correlated with the bulk and surface modes, we varied the antisymmetric surface plasmon energy (ω_{s-}) as a parameter. It was found that only when it was in the range 8.5–9.0 eV, reasonable values for the dielectric-function parameters were obtained. In the next step, we allowed finite lifetimes (nonzero δ_j), and adjusted all seven parameters, by a numerical fit of the loss function (4), to the experimental spectrum. Only small modifications of the initially found parameters, were obtained during this stage.

As shown in Fig. 3(a) the agreement with the experimental spectra is very good, provided that the experimental background is subtracted. An alternative way to eliminate the broad background (taking the risk of enhancing additional weak contributions) is to compare the second derivatives, as shown in Fig. 3(b). Both the intensity and its second derivative are successfully reproduced, indicat-

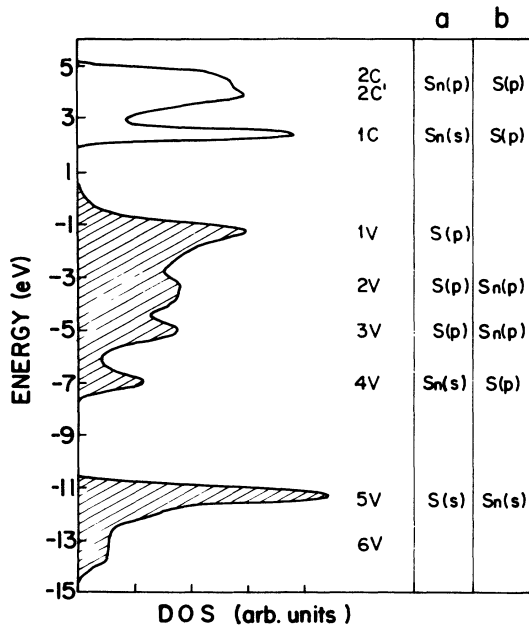


FIG. 2. The valence and conduction DOS functions of SnS₂, as per Simunek (Ref. 37) and Bordas (Ref. 18), respectively. (a) Dominant and (b) secondary orbital characteristics are indicated.

TABLE I. Parameters used in the calculation of the $E_0=2$ -keV loss function (in eV). The superscript asterisk represents dimensionless values.

ω_{p1}	ω_{p2}	ω_{n1}	ω_{n2}	δ_1	δ_2	D^*
16.6	6.7	3.0	10.2	6.0	1.0	4.0

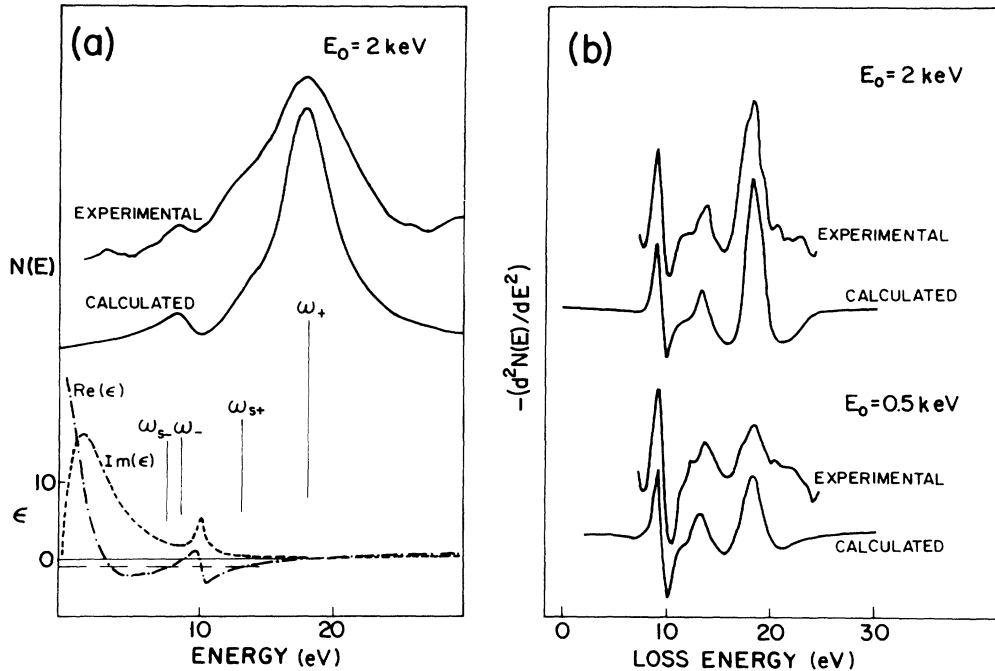


FIG. 3. (a) Top, calculated and measured loss intensities at $E_0 = 2$ keV; bottom, calculated dielectric function. The bisecting points of $\text{Re}(\epsilon)$ with 0 and -1 are indicated. (b) Calculated and measured second derivatives of the loss intensity for $E_0 = 2$ and 0.5 keV.

ing that the 8–20-eV region is fully described by the above function. In particular, it demonstrates that the broad shoulder around 11.0 eV is just a result of the differentiation and is not related to an additional excitation.

The success in predicting, simultaneously, the bulk and surface frequencies supports this model, since the experimental observation shows a value higher than the regular $\omega_p/\sqrt{2}$, expected for a single mode. Moreover, the lower surface mode ω_{s-} is theoretically obtained very close to its bulk parent ω_- , 0.2 eV lower, being unresolved due to the width of the lines. Exactly the same behavior is obtained from the dielectric function of Bertrand *et al.*,¹⁴ deduced from optical-reflectivity measurements.

In addition, the relatively low intensity of ω_- compared with that of ω_+ is straightforwardly obtained, as demonstrated by the $N(E)$ fit. Second-derivative reproduction, below $E_0 = 500$ eV, is, however, more difficult to achieve, even when all the parameters are allowed to vary. This fact results from the inherent dependence of second-derivative intensities on widths. Figure 1(b) shows that for lowered E_0 , the symmetric bulk and surface lines monotonically broaden, while the 9.0-eV linewidth remains roughly constant. Variations of δ_j cannot account for this effect, since both δ_1 and δ_2 influence each of the combined modes: ω_+ and ω_- . Indeed, this reflects the inconsistency of using phenomenological damping parameters to account for different broadening processes occurring on a microscopic scale, such as the already mentioned anisotropy and band dispersion.

The collective nature of the 9.0-eV line is verified by noting that the real part of the dielectric function vanishes around 9.0 eV, while the imaginary part goes through a minimum [Fig. 3(a)]. On the contrary, the neighboring interbandlike transition at 10.2 eV does not contribute a loss peak at all [although $\text{Re}(\epsilon)$ vanishes there, too]. The energy of the antisymmetric mode is, in fact, very sensitive to ω_{n2} , but its plasmonic nature is apparent.

We stress the physically different interpretation of the low-energy plasmon, suggested here to originate from the two plasmas, rather than a single one (frequently assigned to the π band), as widely claimed.^{3,28,40,42} The former approach usually predicts an excessively high plasmon frequency, and attributes the lower experimental value to the influence of neighboring interband transitions. Here, the finite binding energies have an opposite effect, raising ω_- from zero to the experimental value. Since both approaches use the same expression for the dielectric function, it is easy to verify, by varying the parameters, that the present interpretation is the correct one.

In fact, it is found that the oscillation amplitude of ω_- is dominated by the second plasma, rather than the first one, providing further evidence against the ω_π assignment. Yet, the contribution from the first plasma is significant. When the obtained parameters are introduced to the original equations of motion, one finds that $X_+ \approx 1$ and $X_- \approx -2.5$; where X is the relative oscillation amplitude of the two plasmas, $X = X_2/X_1$.

For lower primary energies, calculations were done with the same ω_{pj} and ω_{nj} parameters. The value of D

[Eq. (4)] was found to closely follow a $\sqrt{E_0}$ dependence, provided that the phenomenological widths were properly adjusted, a condition which reliably held for $E_0 > 400$ eV. This result is in remarkably good agreement with the penetration depth (L) in the corresponding region. Semi-classical³⁸ and quantum-mechanical³⁹ considerations suggest for the loss intensity

$$I \sim S \operatorname{Im} \left[-\frac{1}{(\epsilon+1)} \right] + L B \operatorname{Im} \left[-\frac{1}{\epsilon} \right], \quad (4a)$$

where

$$S = E_1^2 / \hbar \omega E_0,$$

$$E_1 \approx 13.6 \text{ eV},$$

and

$$B = \ln(E_1 E_0 / \hbar \omega) / E_0.$$

Since B/S yields only a weak $\ln(E_0)$ dependence, one expects $D = LB/S$ to maintain the $L(E_0)$ relation, as verified experimentally.

It should be noted that we use here the long-wavelength dielectric function, $\epsilon(q \rightarrow 0)$, which is a good approximation for the high- E_0 spectra. One may estimate the influence of the nonzero q contributions by considering the dielectric function within the hydrodynamic approximation. We have found that for $E_0 > 400$ eV, the present results remain basically unchanged.

Finally, we are able to explain, at least qualitatively, the weak dependence on primary energy of the 9.0-eV loss intensity resulting from the overlap of the bulk and surface antisymmetric modes. Angular-resolved REELS of graphite⁴⁰ also shows some strong surface properties of the 7-eV plasmon, in close similarity to the present ω_- . We expect that the angular properties of ω_- in SnS₂, which are not measurable in our system, will be found roughly the same as those of the so-called ω_π of graphite.

The model used here is isotropic, while it is conceivable that the layered structure should lead to some anisotropy. Recalling that a continuous crossover between the xy plane and the z direction is caused by the CMA, it is interesting to check whether the large difference, found experimentally in the widths of the plasmon lines, can be explained by allowing some anisotropy of the parameters while still remaining within the simple macroscopic framework.

In general, any increase in each of the width parameters δ_j results in the broadening of both ω_- and ω_+ (and, consequently, ω_s). On the other hand, variations in the effective masses m_j^* lead to an extremely different broadening of the two lines: For the symmetric-mode energies a downward shift results from any increase of each or both of the effective masses, following the changes projected on ω_{pj} . The corresponding shifts of the antisymmetric modes are, however, negligible. This fact further supports the association of the large value, already calculated for δ_1 , with anisotropy, rather than lifetime.

As for binding energies, one may deduce that ω_{n2} , which strongly influences the value of ω_- , is roughly iso-

tropic. This conclusion is supported by the correspondence of our results to in-plane q data, suggesting that ω_- does not shift with the direction of the wave vector.

The calculated parameters, given in Table I, indicate an additional point: ω_{pj} are, in fact, consistent with the partial occupation of the two bands presented in Fig. 2. However, the binding energy ω_{n2} is too low to be related to the deep valence band (5V-6V). In principle, the microscopic expression of the dielectric function suggests that ω_{nj} should be identified with allowed single-electron transitions, rather than peaks in the DOS function. Indeed, it is found that ω_{n2} coincides with an intensive peak of the joint DOS.^{14,15,18} This leads to the conclusion that the plasmas cannot be simply identified with the ground-state electronic configuration, as attempted in previous works,^{3,28,33} but rather with electrons that participate in certain electronic transitions.

The simplicity of the two-plasma model is an important advantage in demonstrating the nature of the 9.0-eV loss. We can, of course, extend our calculations by taking a more detailed band structure. In Fig. 4 we show an experimentally deduced dielectric function,¹⁴ in comparison with a function calculated with six plasmas [a

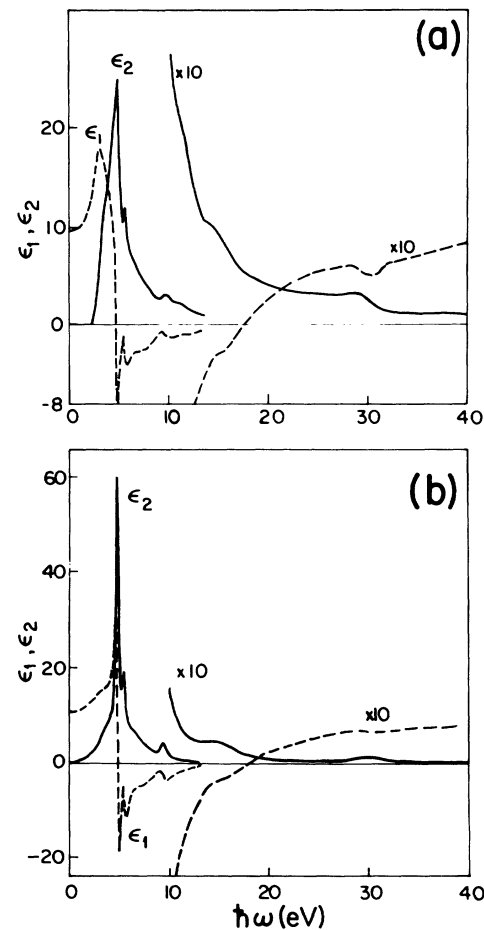


FIG. 4. The dielectric function, real (ϵ_1) and imaginary (ϵ_2) parts: (a) deduced from reflectivity measurements, as per Bertrand *et al.* (Ref. 14); (b) calculated with seven plasmas.

seventh term was also included for the description of the transitions from the Sn(4*d*) levels, discussed in Sec. IV]. This dielectric function gives, at the correct frequencies, all the additional low-energy-loss peaks, which were completely absent from the two-plasma calculations. Also, the binding-energy parameters ω_{nj} again coincide with the measured peaks of the single-electron transitions. On the other hand, the calculated loss intensities are incompatible with the experimental ones, especially when fit is done for the second derivative. This is, again, the consequence of describing different broadening processes by a single parameter— δ .

Typically, all the low-energy peaks are associated with a behavior of the dielectric function, which is similar to that obtained for the 9.0-eV loss: They appear around minima of $\text{Im}(\epsilon)$ and zeros of $\text{Re}(\epsilon)$, where plasmonic solutions are allowed. Previous publications have mentioned already the “shift” of loss peaks, relative to calculated, and optically measured, single-electron transitions,^{29,43,44} but did not give a satisfying physical explanation for such shifts. We claim that the correspondence of loss peaks to reflectivity minima (and vice versa), is a result of the technique’s sensitivity to different excitations: The loss peaks are, in general, of a significant collective nature. They may be coupled to close interband

transitions, but always tend to appear in gaps of the joint DOS. In fact, this interpretation is very appealing, since the number of eigenmodes should be related to the number of plasmas introduced into the model. In the present case, this interpretation is verified by the coincidence of the loss minima at 4.9, 5.7, 7.5, and 10.2 eV with the major maxima of the reflectivity spectra.^{13–15}

Applying the present calculations to MoS₂, for example, a material having a very similar total-valence-band-DOS function,³⁷ we obtained, again, a fairly good agreement with the published loss functions.³⁶ It is believed that many of the dichalcogenides have similar properties, and probably graphite, too.

B. Transitions from the Sn(4*d*) core levels

The transitions originated at the Sn(4*d*) core levels are well observed in the 25–30-eV range. Using a high-energy-resolution mode, we verify the split of the main doublet of lines [see $N(E)$ in Fig. 5] into a more complex structure (second derivative in Fig. 5): at least five lines are resolved throughout this region, while additional related signals are observed above 30 eV. The dominant band, which consists of two major lines at 29.9 and 28.9 eV, and two weak ones at 30.8 and 28.1 eV, excellently fits the reflectivity spectrum of Bertrand *et al.*¹⁷

Less clear is the correspondence within the lower range, where two well-resolved peaks at 26.7 and 25.5 eV are obtained. Referring again to the above reflectivity spectra,¹⁷ it is obvious that corresponding signals, although observable, are weaker. On the other hand, their comparable line at 27.5 eV hardly appears in our measurements.

One may question the coincidence of loss peaks with reflectivity peaks, in view of the above discussion. Certainly, since $\text{Re}(\epsilon)$ is included in the loss function, screening effects exist inherently in the loss peaks. However, in the present energy region, one finds that $\text{Re}(\epsilon)$ is close to unity, with rather weak variations around the transition energies.^{14,18} The loss peaks coincide, therefore, with maxima, rather than minima of $\text{Im}(\epsilon)$, in contrast with the low-energy region. Indeed, as mentioned above, we included in Fig. 4 a representative seventh term to account for the Sn(4*d*) transitions. We have found that the shift of the relevant loss peak, with respect to $\text{Im}(\epsilon)$, does not exceed 0.1 eV. This is, in fact, a typical case of core-level transitions: The collective character of their related loss peaks is dramatically reduced, as expected from the localization of the initial state. In fact, the localization in the present case is even more pronounced due to the final states involved, a point which is discussed below.

In Figs. 6(a)–6(c) several DOS calculations of the conduction bands are presented. Despite some significant discrepancies, we stress that a general agreement on the character of these bands does exist: the lowest peak (labeled here as 1C) is dominated by Sn(*s*) states, with minor S(*p*) contributions, while 2C' and 2C are mainly Sn(*p*) states (see also Fig. 2). Relying on these results, one can interpret the observed signals, taking into account the splitting of the core level, which has been determined by

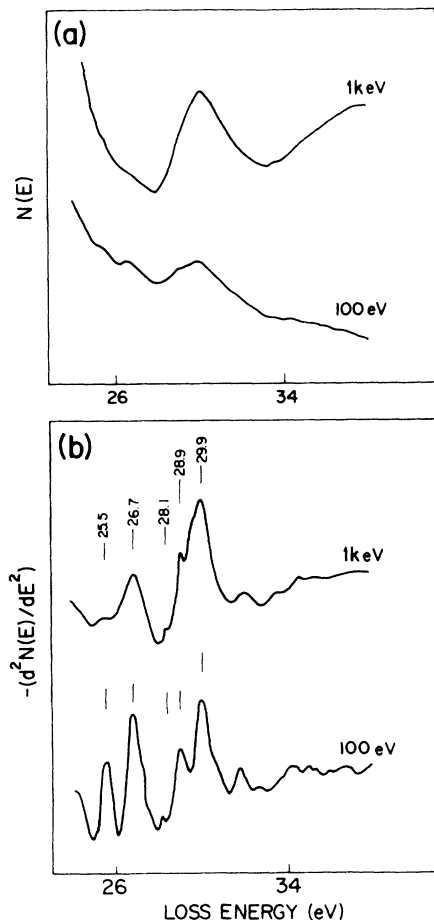


FIG. 5. Loss spectra of the Sn(4*d*) core-level transitions: (a) intensities; (b) second derivatives.

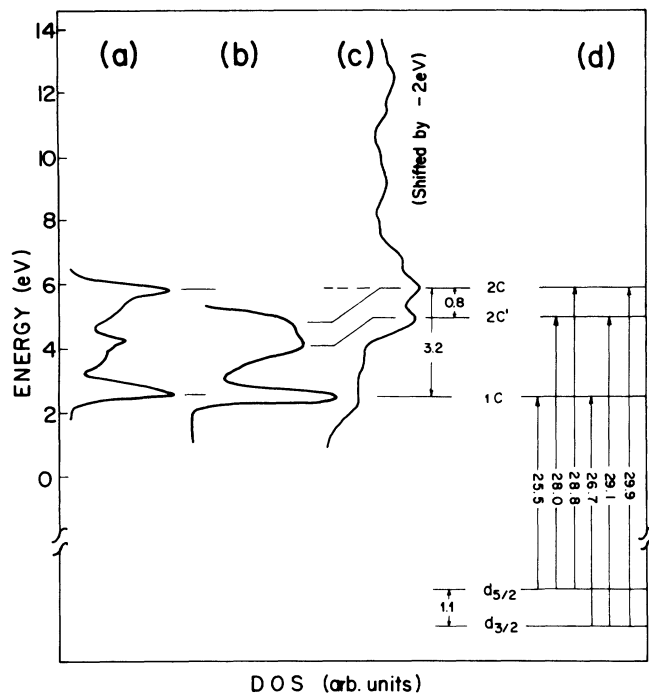


FIG. 6. A comparison of several calculated conduction-band DOS functions, relative to the top of the valence band, as per (a) Robertson (Ref. 6); (b) Bordas (Ref. 18); (c) Margaritondo (downwardly shifted by 2 eV) (Ref. 22). (d) A schematic illustration of electronic transitions from the Sn(4d) levels, as derived from the present experiments.

XPS to be about 1.1 eV, in agreement with reported values¹⁷ for the $j = \frac{5}{2}$ and $\frac{3}{2}$ levels. It is worthwhile recalling that the partial p -type final DOS is actually measured, since the d initial states are not k dispersive, and the cross section is, therefore, proportional to the density of the odd-parity final states.

The dominant line is, therefore, naturally attributed to the transitions terminated at 2C (and 2C'), while the minor p -like contribution in 1C enables the weak appearance of the lower couple of lines. A 3.2-eV separation between 1C and 2C, with 2C' positioned at about 0.8 eV below 2C, and a 1.1–1.2-eV split of the core levels are consistent with our experimental data [see Fig. 6(d)]. The $d_{3/2}$ to 2C' transition at 29.1 eV is unresolved from the $d_{5/2}$ to 2C line at 28.8 eV.

The mentioned band calculations partially agree with the present assigned values. Our 1C-2C separation is consistent with those obtained by Margaritondo *et al.*²² and Robertson,⁶ while the 2C and 2C' difference is obtained by Margaritondo *et al.* and by Bordas, Robertson, and Jakobsson.¹⁸ The sharp 1C peak in Refs. 14 and 18 seems to resemble the experimental narrow 26.7- and 25.5-eV lines. This, however, does not contradict the broad peak in Ref. 22, since the partial DOS only is experimentally measured here.

On the other hand, absolute transition energies are totally different from the expected ones. When the core-

level energies, 24.4 and 25.5 eV below the valence-band top, are adopted from UPS data,^{17,41} a shift of about 1.5 eV is needed to correlate between measured and calculated values. This shift is consistent with the measured threshold at 25.0 eV, noting that 26.6 eV is expected for a band gap of about 2.2 eV (at room temperature).¹²

We believe that the determination of the threshold by Bordas *et al.*¹⁷ is erroneous because of the low intensities of the optical transitions to 1C, while the present threshold value is consistent with the easily determined peaks mentioned above. The advantage of the present technique, demonstrated here, is twofold: typical high cross sections, enabling a common use of derivatives to emphasize weak signals, and the relaxation of selection rules, which results in higher intensities of the parity-forbidden transitions, especially at low E_0 (see Fig. 5).

A reasonable explanation of the difference between experimental and theoretical transitions is, as previously proposed,^{17,18,27} the existence of strong e - h interactions. In the present case, both the final, and certainly the initial, states are well localized near the Sn atom, giving rise to enhanced correlation effects.

Alternatively, one may relate these transition values to impurity states within the energy gap. This, however, is not expected to be relevant, since such levels should also show up in the low-losses region. Furthermore, the presence of such impurity levels would introduce additional lines, rather than shift the expectedly strong interband transitions.

The present measurements prove, therefore, the existence of excitonic states with huge binding energy, of the order found in PbI_2 and PbI_3 .^{36,45} Although expected to be small in this region, we recall the typically upward energy shift of REELS as well as reflectivity signals, relative to $\text{Im}(\epsilon)$ and the corresponding calculated transitions. With such a shift, the actual discrepancy with the calculated transitions is even larger.

To verify the above values, we next compare our results with other experimental data. The combination of BIS and CIS can provide, in principle, a complete picture of the unoccupied DOS function. Moreover, excitonic effects are not expected to be reflected in BIS, where the electron transition takes place between two unoccupied levels, nor in CIS, in which the measured scattering processes involve delocalized final states only. Classically, this means that in CIS the detected photoelectron must escape far from the hole, carrying no information about bound excitonic states. Therefore, it is clear that the comparison between the two techniques and EELS is a useful method for the quantitative study of correlation effects.

Applied to SnS_2 ,^{23,27} results of these techniques are found consistent, but shifted upward by about 3 eV compared to our results (and to reflectivity). The sign of the relative shift is a further indication of the existence of excitonic effects in this compound. Yet the value of 3 eV for the binding energy, deduced from these experimental results, is extremely large. The value of 1.5 eV, obtained from comparison with the calculations in Refs. 6 and 18, seems to be much more plausible, in view of what is known for other related compounds.³⁶ Probably, the

conduction-band DOS obtained by Margaritondo *et al.*²² is shifted upward. An additional evidence for that is found in the low-energy-loss region: their prediction of 1C at about 4.2 eV above E_V (indicating a first peak above 5.5 eV) is inconsistent with our 3.8-eV-loss peak. Moreover, the difference between the two values is close to the difference in the predicted excitonic binding energies.

Bordas, Robertson, and Jakobsson¹⁸ have raised the question of the relevance of single-electron band calculations when extremely large correlation effects exist. Yet the present results can account for the calculated conduction-band structure, provided that a downward shift, related to the excitonic binding energy, is taken into account.

Considering intensities, one finds the transition from the $4d_{3/2}$ to 1C to be much more intensive than that from the second core level. This suggests that the 1C level is dominated by $j = \frac{1}{2}$ states. Similarly, the dominant intensity of the 29.9-eV line indicates a mixture of $p_{3/2}$ and $p_{1/2}$ states in 2C, since pure $p_{3/2}$ states lead to stronger intensity of the transition from $d_{5/2}$. Consequently, we believe that the bound excitonic states consist of hybridized levels.

Higher-energy structures in the conduction DOS can be observed above the 30-eV loss. The peaks at about 32.0 and 30.8 eV, at 34.7 and 33.6 eV, and at 37.5 and 36.5 eV may be assigned to 3C, 4C, and 5C final states, respectively. These roughly support the *f*, *g*, and *h* structures obtained by CIS.²² In this spectral region, low primary energies are preferred, due to the reduced intensity of the second harmonic of the 18.7-eV plasmon.

At low primary energies, the relative intensity of the transitions to 1C are considerably enhanced (see the relative intensities in Fig. 5). This effect is attributed to the relaxation of the optical selection rules, resulting in the enhancement of transition matrix elements to 1C, which is dominated by *s*-type orbitals.

IV. SUMMARY

Reflection EELS of SnS₂ up to 40 eV has been presented and interpreted, with comments on several complementary studies of this system. Several aspects of the

technique capabilities are examined, especially the sensitivity to excitation of complex collective modes.

The present results are essentially consistent with the existing band-structure data of SnS₂, but reveal some discrepancies concerning the conduction-band energies, which indicate the importance of electron correlations. It is found that excitons, associated with the Sn(*4d*) core level, have extremely large binding energies, determined to be about 1.5 eV. This value is much higher than 0.4 eV suggested by a previous reflectivity study,¹⁷ but is lower than the value derived from the comparison of that reflectivity study with BIS experiments.²⁷ Probably, these excitons are related to bound states of an atomic size. A roughly rigid shift of the lowest conduction bands can account, however, for our experimental data.

Using a simple two-plasma model, we have demonstrated some general features of the low-energy-loss structures. It has been shown that loss peaks, traditionally attributed to single-electron transitions, have a collective character. The various plasmons can be alternatively considered as the eigenmodes of interacting plasmas, enhanced within the gaps of the single-electron transitions.

This interpretation emphasizes the physically different origins of the loss and the optically measured peaks, reflected also in their appearance at different energies. Furthermore, it clarifies the different properties of the various modes, such as their surface character and their linewidths.

The macroscopic approach used here is very successful in quantitatively accounting for the loss frequencies, as well as for the loss intensities. However, it is limited in describing broadening processes, and dispersion in particular. Further investigation is necessary to clarify the microscopic origin of the broadening effects.

ACKNOWLEDGMENTS

We would like to thank Dr. M. Kapon for the thorough x-ray analysis and assistance. This research has been supported in part by the VPR and R. Biss Metallurgy Research Funds.

¹Y. Ohno, Phys. Rev. B **39**, 8209 (1989).

²Y. Ohno, Phys. Rev. B **36**, 7500 (1987).

³T. Ito, M. Iwami, and A. Hiraki, J. Phys. Soc. Jpn. **50**, 106 (1981).

⁴Y. Ohno, Solid State Commun. **67**, 1089 (1988).

⁵B. Palosz, Acta Crystallogr. Sect. C **42**, 653 (1986); B. Palosz, W. Steurer, and H. Schulz, *ibid.* **B 46**, 449 (1990).

⁶J. Robertson, J. Phys. C **12**, 4753 (1979).

⁷M. J. Powell, E. A. Marseglia, and W. Y. Liang, J. Phys. C **11**, 895 (1978).

⁸I. Ch. Schluter and M. Schluter, Phys. Status Solidi B **57**, 145 (1973).

⁹C. Y. Fong and M. L. Cohen, Phys. Rev. B **5**, 3095 (1972).

¹⁰M. Y. Au-Yang and M. L. Cohen, Phys. Rev. **178**, 1279 (1969).

¹¹R. B. Murray and R. H. Williams, J. Phys. C **6**, 3643 (1973).

¹²M. J. Powell, J. Phys. C **10**, 2967 (1977).

¹³D. L. Greenaway and R. Nitsche, J. Phys. Chem. Solids **26**, 1445 (1965).

¹⁴Y. Bertrand, G. Leveque, C. Raisin, and F. Levy, J. Phys. C **12**, 2907 (1979).

¹⁵C. Raisin, Y. Bertrand, and J. Robin, Solid State Commun. **24**, 353 (1977).

¹⁶J. Camassel, M. Schluter, S. Kohn, J. P. Voitchovsky, Y. R. Shen, and M. L. Cohen, Phys. Status Solidi B **75**, 303 (1976).

¹⁷Y. Bertrand, G. Leveque, J. Robin, and R. Mamy, Physica B **99**, 287 (1980).

¹⁸J. Bordas, J. Robertson, and A. Jakobsson, J. Phys. C **11**, 2607 (1978).

¹⁹C. Raisin and Y. Bertrand, J. Phys. C **15**, 1805 (1982).

- ²⁰U. Berg, T. Chasse, and O. Brummer, *Phys. Status Solidi B* **108**, 507 (1981).
- ²¹C. A. Formstone, E. T. FitzGerald, P. A. Cox, and D. O'Hare, *Inorg. Chem.* **29**, 3860 (1990).
- ²²G. Margaritondo, J. E. Rowe, M. Schluter, and H. Kasper, *Solid State Commun.* **22**, 753 (1977).
- ²³G. Margaritondo and J. E. Rowe, *Phys. Rev. B* **19**, 3266 (1979).
- ²⁴U. Berg and T. Chasse, *Phys. Status Solidi B* **135**, 633 (1986).
- ²⁵W. Jaegermann, F. S. Ohuchi, and B. A. Parkinson, *Ber. Bunsenges. Phys. Chem.* **93**, 29 (1989).
- ²⁶D. O'Hare, W. Jaegermann, D. L. Williamson, F. S. Ohuchi, and B. A. Parkinson, *Inorg. Chem.* **27**, 1537 (1988).
- ²⁷Y. Gao, B. Smandek, T. J. Wagner, J. H. Weaver, F. Levy, and G. Margaritondo, *Phys. Rev. B* **35**, 9357 (1987).
- ²⁸W. Y. Liang and S. L. Cundy, *Phylos. Mag.* **19**, 1031 (1969).
- ²⁹Y. Ohno, *J. Phys. Soc. Jpn.* **59**, 3740 (1990).
- ³⁰H. Cohen, Z. Esterlit, R. Brenner, E. Lifshitz, T. Maniv, and M. Folman, *Mater. Sci. Forum* **91-93**(2), 733 (1992).
- ³¹E. Doni and R. Girlanda, in *Electronic Structure and Electronic Transitions in Layered Materials*, edited by V. Grasso (Reidel, Dordrecht, 1986).
- ³²F. S. Ohuchi, B. A. Parkinson, K. Ueno, and A. Koma, *J. Appl. Phys.* **68**, 2168 (1990).
- ³³H. Raether, in *Excitation of Plasmons and Interband Transitions by Electrons*, edited by G. Höhler, Springer Tracts in Modern Physics Vol. 88 (Springer, Berlin, 1980).
- ³⁴R. Manzke, J. Fink, and G. Creselius (private communication); See also E. Tosatti and R. Girlanda, in *Electronic Structure and Electronic Transitions in Layered Materials* (Ref. 31).
- ³⁵E. Tosatti and R. Girlanda, in *Electronic Structure and Electronic Transitions in Layered Materials* (Ref. 31).
- ³⁶A. Balzarotti and M. Piacentini, in *Electronic Structure and Electronic Transitions in Layered Materials* (Ref. 31).
- ³⁷A. Simunek and G. Wiech, *Phys. Rev. D* **30**, 923 (1984).
- ³⁸R. H. Ritchie, *Phys. Rev.* **106**, 874 (1957).
- ³⁹A. A. Lucas and M. Sunjic, in *Fast Electron Spectroscopy of Collective Excitations in Solids*, edited by S. G. Davidson, Progress in Surface Science Vol 2, Pt. 2 (Pergamon, New York, 1972).
- ⁴⁰U. Diebold, A. Preisinger, P. Schattschneider, and P. Varga, *Surf. Sci.* **197**, 430 (1988).
- ⁴¹F. R. Shepherd and P. M. Williams, *J. Phys. C* **7**, 4416 (1974).
- ⁴²A. Koma and K. Yoshimura, *Surf. Sci.* **174**, 556 (1986).
- ⁴³L. Papagno and L. S. Caputi, *Surf. Sci.* **125**, 530 (1983).
- ⁴⁴E. Colavita, M. De Crescenzi, L. Papagno, R. Scarmozzino, L. S. Caputi, R. Rosei, and E. Tosatti, *Phys. Rev. B* **25**, 2490 (1982).
- ⁴⁵G. Margaritondo, in *Electronic Structure and Electronic Transitions in Layered Materials* (Ref. 31).